45th AIAA/ASME/ASCE/AHS/ASC Structures, Structural Dynamics & Materials Conference
19 - 22 April 2004, Palm Springs, California

AIAA 2004-2051

STIFFENED PANELS IN COMPRESSION: REDIRECTING LOADS TOWARD HIGH-STRENGTH STIFFENERS

Sjoerd van der Veen, Alcan Aerospace, corresponding author
sjoerd.van.der.veen@alcan.com

Daniel Coatta, University of Michigan

Abstract

New skin alloys are being developed that are both damage tolerant and strong in compression. At the same time, stiffener alloys are still getting stronger. Stiffened panel designs need to be optimized in new ways to fully benefit from these new material properties. FEA has shown that, provided the joint between skin and stiffeners is good and stringers are strong enough, the overall efficiency of a stiffened panel with large attach flanges is greater than that of a panel which has very high quadratic section moment. Stringer pitches can thus be kept at economic levels while panel buckling performance is increased by the use of new higher strength, high damage tolerance skin and the next generation of high strength stiffeners.

The tangent modulus curves of the new materials mentioned are generally steeper than those of current materials. The present analyses have demonstrated that because the strain in a post-buckled stiffened panel is far from uniform, this does not present any particular risks with respect to sudden loss of stiffness of the panel.

Introduction

The design of stiffened airframe panels is driven by three major factors. First, the panels must frequently support large compressive loads. Second, the skin of the panels must often be highly damage tolerant. Finally, the stiffeners should be spaced as far apart as possible to decrease the cost of panel production.

New skin alloys are being developed that are both damage tolerant and strong in compression. Stiffened panels will have to be re-optimized to make full use of the higher-strength skin. Based on current methods of panel design, this optimization would simply lead to reduced skin thickness and more closely spaced stiffeners. Reduction in thickness will lead to reduced stiffener spacing because the panel's elastic skin crippling stress, which is proportional to the square of the ratio of the skin thickness to the stiffener spacing. The elastic crippling stress is given by the formula [1, 2]:

$$f_{crippling,elastic} = \frac{k\pi^2 E}{12\left(1-\nu^2\right)} \cdot \left(\frac{t}{b}\right)^2, \qquad (1)$$

where

- $f_{crippling,elastic}$ is the elastic crippling stress of the skin
- k is the edge restraint constant
- E and ν are material constants
- t is the skin thickness and b is the stiffener spacing

Although post-buckling design allows for local skin crippling at loads lower than the ultimate limit load, the skin crippling stress cannot be greatly reduced without increasing the risk of fatigue problems in the skin-stiffener joint.

The strength of extruded aerospace stiffeners is also increasing. Twenty years ago, 7175-T73511, with its compressive yield strength (F_{cy}) of 410 – 450 MPa (59 – 65 ksi), was widely used. Today's standard for riveted fuselage shells is 7349-T76511, with an F_{cy} of 570 – 600 MPa (84 – 87 ksi). The next generation of stiffener alloy, already under development, has a target F_{cy} of at least 700 MPa (100 ksi). Since for these products, there is less need to balance strength with damage tolerance, the stiffeners are usually the strongest components in a stiffened panel.

New stiffened panel designs will therefore also need to account for increased stiffener strength. A design that seeks a high Euler buckling resistance – as opposed to a high post-buckling resistance – would maximize the quadratic section moment (i.e. minimize the section of the attach flange). The high strength of present-day stiffeners would likely lead to a reduction of the gauge of the stiffener web fastened flange(s). This reduction would be possible because local crippling stresses would be high even when corrected for plasticity effects. Although this design strategy would produce a stiffened panel with a high Euler buckling stress, the stiffeners in such a panel would provide little edge restraint to the skin. As a result of this, a design that accounts only for Euler buckling is sub-optimal in post-buckling.

Objective of Present Work

To produce optimal results, a panel design must account for post-buckling performance. The objective of the present work is to propose a new design for a generic stiffened panel that makes full use of the strength of next-generation stiffeners. The hypothesis that is at the basis of this work is that the most efficient design will meet two major goals:

- Efficiently redirect load from the buckled skin to the stiffeners in order to take advantage of their high strength and to ensure that the panel has a high post-buckling strength
- Support and provide edge restraint for the skin in order to postpone the onset of local skin crippling and to allow for the use of thinner, higher-strength skin without unduly decreasing stiffener spacing

The first goal could be achieved by maintaining a high stiffening rate for the panel. The stiffener cross-section should therefore not be minimized, even if the local buckling stresses in the stiffener's section are very high.

The second goal could be met by using the fastened flange as an edge restraint for the skin. In addition to delaying the onset of skin pocket buckling, this approach helps accomplish the first goal by increasing the efficiency of the load transfer from skin to stiffeners once pocket buckling occurs.

When these solutions are implemented, the joint between the skin and the stiffeners becomes crucial. Although bonding would seem to be the best fastening method, modern welding techniques like laser-weld bonding and lap-friction stir welding may be worth investigating.

Idealized Euler-Johnson and finite element analyses (FEA) have shown that this new panel design strategy permits wide spacing between stiffeners. Therefore, a stiffened panel with adequate post-buckling performance has the potential to satisfy the three design criteria of compressive strength, damage tolerance, and acceptable production cost.

A further objective of the present work is to recall the differences between a stiffened panel and a beam-column. The tangent

modulus curves of the alloys studied (Figure 1) are all much steeper than those of more conventional alloys such as 2024 or 7x75. One could be led to think that stiffeners with such steep tangent modulus curves could absorb only very limited deformation before collapsing entirely. However, the "deformation" in this context is the *average* deformation of the panel. For a stiffened panel, this is only an artificial concept, which allows the use of adapted beam-column analysis methods to predict compression stability. In reality, the strains in a post-buckled stiffened panel show considerable gradients. It will be shown that these contribute to a benign buckling behavior even if tangent modulus curves are steep.

Approach

The new design approach was verified using Euler-Johnson empirical/analytical calculations and FEA. As a baseline, a T-section integral stiffener design was chosen, representative of laser-welded fuselage shells. Z- and I-section alternatives were also investigated, using varying stiffening rates and stiffener materials. Figure 1 shows the stress-strain curves of three materials used in these simulations.

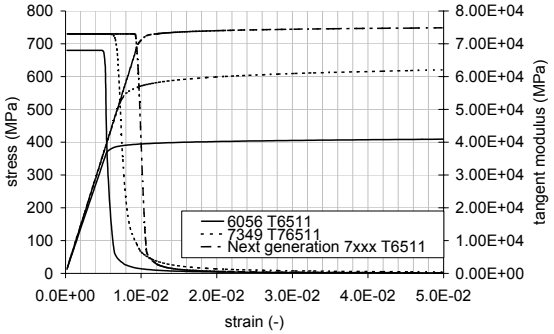

Figure 1: Stiffener properties used in both finite element simulations and Euler-Johnson calculations (stress-strain and tangent modulus curves)

For simplicity, the properties of 6056-T6511 were used for the skin in all models because they approximate the properties of a next-generation weldable and damage-tolerant fuselage skin.

Approach – Euler-Johnson Analyses

The Euler-Johnson method was used as an illustration of an analytical-empirical sizing method that is still widely used today. It uses one of two models (Euler or Johnson) to determine the buckling stress of a column. If the column is slender – a panel with a large frame spacing, for example – it buckles as an Euler beam-column, and the buckling stress is given by the equation

$$f_{crit} = \frac{\pi^2 E}{\left(\frac{L'}{\rho}\right)^2}, \qquad (2)$$

where

- f_{crit} is the column buckling stress
- L' is the effective column length (=(L/e), where L is the column length and e is the end fixity factor)
- ρ is the radius of gyration (=√(I/A), where I is the quadratic section moment and A is the section area)

For the present analysis, the column was modeled as simply supported, with a fixity factor of 1.

A second model must be used if the column is less slender than $\sqrt{(2\pi^2 E/f_{crippling})}$. In this case, the thin-walled section will distort before the entire column buckles; local crippling of the skin and stiffeners will occur. The equation for this regime of buckling is

$$f_{crit} = f_{crippling}\left[1 - \frac{f_{crippling}\left(\frac{L'}{\rho}\right)^2}{4\pi^2 E}\right], \qquad (3)$$

where

- $f_{crippling}$ is the crippling stress of the panel, a.k.a. the stress at zero slenderness

The crippling stress of a thin-walled section is the weighted average of the crippling stresses of the individual strips and corners that make up the section.

There are several ways of computing $f_{crippling}$:

1. Empirical equations derived by Needham, Gerard, or Niu can be used to determine the crippling stresses of subsections, such as one half of a Z-stiffener (angle section) [1,2]
2. Equations derived from plate theory such as Equation 1, with appropriate edge restraint factors

For the present analysis, the second way of computing $f_{crippling}$ was used. Stiffener webs were modeled as infinitely long[1] and clamped on both edges, with an edge restraint factor of 6.98. Flanges were modeled as clamped on one wide but free on the other, with an edge restraint factor of 0.43. The skin was modeled as infinitely long and simply supported on all edges, with an edge restraint factor of 4 [1, 2].

To use the Euler-Johnson method in true post-buckling design, the panel must be modeled as a column comprising the stiffeners and only part of the skin. The width of this load-bearing portion of the skin is called the effective skin width. This concept accounts for the early buckling of portions of the skin that are not strengthened by stiffeners. Various methods exist to compute b_{eff}, the effective skin width:

1. $b_{eff} = \text{constant} \cdot t$ (4a)

2. $b_{eff} = t\sqrt{\frac{KE}{F_{cy_{skin}}}}$ [1], (4b)

   where
   - K is a fixity factor
   - E is the Young's modulus of the skin material
   - $F_{cy,skin}$ is the compressive 0.2% proof stress of the skin material

3. $b_{eff} = t\sqrt{\frac{KE}{F_{cy_{stiffener}}}}$ [1], (4c)

   where
   - $F_{cy,stiffener}$ is the compressive 0.2% proof stress of the stiffener material, accounting for the fact the stresses in the post-buckling range may exceed $F_{cy,skin}$

4. $b_{eff} = t\sqrt{\frac{KE}{F_{crippling,stiffener}}}$ [2], (4d)

   where
   - $F_{crippling,stiffener}$ is the crippling stress of the stiffener alone, accounting for the fact that the stiffener crippling stress will likely be lower than $F_{cy,stiffener}$

For the present analysis, the fourth method was used. A more advanced method still would be to replace the stiffener crippling stress in the fourth method with the crippling stress of the entire panel. An iteration loop would then be required to solve for b_{eff} and $f_{crippling}$.

[1] If the pocket or strip is "infinitely long," the wavelength of its buckling mode is much smaller than the length of the pocket or strip. In such a case, the boundary conditions on the short edges have very little influence.

In post-buckling design, the critical stress of the panel can exceed the proof stresses of the skin and stiffener materials. As a result, calculations must include a plasticity correction. Moreover, skin and stiffener materials may differ significantly, both in the value of the compressive Young's modulus and in the proof stress. The simplest way to account for these issues is to replace all Young's moduli in the above equations with the tangent modulus E_t. For the present analysis, however, slightly more advanced plasticity corrections were implemented to account for plate edge constraints and Poisson's effect. The formulas for these corrections are [2]

$\eta = \frac{1-\upsilon^2}{1-\upsilon_p{}^2} \cdot \frac{E_s}{E}$ for flanges (strips with one of the long edges free) (5a)

and

$\eta' = \eta \cdot \left[\frac{1}{2} + \frac{1}{4}\sqrt{1+\frac{3E_t}{E_s}} \right]$ for skin and stiffener web, (5b)

where

- E_s is the secant modulus
- υ is Poisson's ratio
- $\upsilon_p = \frac{1}{2} - \left(\frac{1}{2} - \upsilon\right)\frac{E_s}{E}$

The stress distribution between skin and stiffeners must be calculated using the secant modulus E_s; skin and stiffeners are like parallel springs undergoing equal deformation, so their respective instantaneous stiffnesses determine their individual stresses. The whole calculation procedure is thus iterative, since the non-linear behavior of E_t and E_s is coupled with the non-linear character of the effective width and the distribution of load between skin and stiffeners.

The constitutive behavior of the materials was modeled in the form of Ramberg-Osgood curves. The ultimate tensile stress F_{tu} was used as a cutoff stress throughout; if a local mode was found to exceed this stress, the stress was cut off at F_{tu}.

Two different sets of Euler-Johnson calculations were performed. In the first, no joint whatsoever was considered between skin and stiffener. Instead, the skin and stiffener were assumed to undergo the same strain. Section properties of the panel were calculated considering both the effective width of the skin and the entire stiffener. The second series of Euler-Johnson calculations modeled a perfect bond between skin and stiffener. This model was accomplished by considering the fastened flanges and the attached skin to be a single strip with an effective thickness given by the equation

$$t_{eff} = \frac{t_{skin}E_{s,skin} + t_{stiffener-flange}E_{s,stiffener}}{E_{s,stiffener}} \quad (6)$$

This effective thickness technique helps approximate a perfect bond between skin and stiffeners. It assumes that the entire bonded section has the same material properties as the stiffener, with the exception of the cutoff stress. To compensate for the weakness of the skin, the assumed thickness of this section is decreased.

The cutoff stress in the bonded section is recalculated using the formula

$$F_{tu,eff} = \frac{F_{tu,skin}t_{skin} + F_{tu,stiffener}t_{stiffener-flange}}{t_{skin} + t_{stiffener-flange}} \quad (7)$$

For both sets of calculations, four stiffened panel cross-sections were studied:

1. T-shaped stiffener, stiffening ratio = $\frac{A_{stiffener}}{A_{stiffener} + A_{skin}} = 0.208$
2. Z-shaped stiffener, stiffening ratio = 0.316
3. Z-shaped stiffener, stiffening ratio = 0.347
4. I-shaped stiffener, stiffening ratio = 0.455

The dimensions for each type of cross-section are shown in Table 1 (end of paper). The panel depth was 609.6 mm in all cases.

Results – Euler-Johnson Analysis

The results of the Euler-Johnson analysis are shown in Tables 2 and 3 (end of paper). Table 2 gives the results of the first set of calculations, while Table 3 shows the results of the second set. A comparison of the two tables leads to several notable observations. First, for panels with Z- and I-section stiffeners, the predicted skin crippling stresses and overall panel strengths are higher in the perfectly bonded model (Table 3). This result is expected, since the stiffener provides more support to the skin in this model.

A second observation from the tables is that the use of stronger material in the stiffeners produces stronger panels. This result holds for both the non-bonded and perfectly bonded models.

A more minor note is that the perfectly bonded model predicts slightly higher buckling stresses for T-section stiffeners. This small discrepancy arises from the algorithm used by the bonded model. Any point of skin-stiffener contact is viewed by this model as a bond. In the case of the T-section stiffeners, the width of the vertical component of the stiffener is assumed to be bonded. The small size of this dimension explains why the T-section buckling stresses are only slightly different in the two tables.

Approach – Finite Element Analyses

Finite element models were created to refine the results of the Euler-Johnson analysis. These models were 7 stiffeners wide, and the skin was given a radius of curvature of 2.9 m, as shown in Figure 2. Loads were introduced to the model by adding half of a frame bay to each side of the panel. Both of these additional sections were constructed of very stiff skin – more than 1000 times stiffer than other parts of the model. This modeling approach was not used for the stiffeners; these had realistic properties over the entire panel length, enabling them to undergo lateral buckling modes with long wavelengths. This design minimized the influence of boundary conditions, producing stable simulations and quick convergence. The nodes of the fastened flanges were linked rigidly to the skin, thus simulating a perfect bond. The non-linear MARC solver was used, with large displacements enabled and automatic time stepping on the displacement control of the end-shortening of the panels (arc length method, Riks-Ramm algorithm). It was not deemed necessary to seed the meshes with any imperfections.

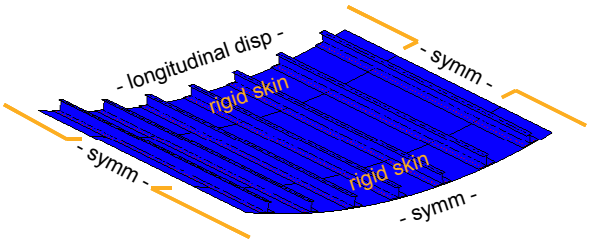

Figure 2: Finite element model of I- stiffened panel

Results – Finite Element Analyses

In the FEA models, all panels showed a benign buckling behavior, with a first mode

of half-wavelength crippling of the skin pocket accompanied by slight stiffener twisting. The T-section stiffened panels developed a second mode, with the skin crippled in one full wave. Collapse always occurred due to the crushing of a third mode, with the skin crippling in one-and-a-half waves and the stiffeners buckling laterally. Figure 3 (end of paper) shows the buckling modes produced by one of the models.

Figure 4 (end of paper) shows the force-displacement diagrams for the FEA models. This figure demonstrates that the panels do not loose all of their stiffness over a very small range of strain. This result supports the previous assertion that alloys with steep tangent modulus curves may be successfully used in the fabrication of stiffened panels. In fact, it is mainly the design that determines the shape of the force-displacement curve. The slope of the tangent modulus curve is not an accurate measure of the rapidity of collapse for these panels.

Table 4 shows the average stresses associated with the first loss of stiffness (an indication of skin crippling) and the ultimate stress calculated using FEA. Note that these should not be compared directly to the stresses predicted using Euler-Johnson, since the FEA included curvature and should therefore be slightly more stable. In the scope of this work, the goal was to compare the stability increase from higher strength stringers and an adapted design, as predicted by each method. It was assumed that these relative results, given in Table 6 (end of paper), were not affected by curvature.

Discussion

The results in Tables 2 – 4 support the hypothesis that wide attach-flanges can greatly increase skin pocket buckling resistance. The panel collapse loads also increase with wide attach flanges, but one has to bear in mind that the sections of the different panels were not equal, as indicated in Table 5 (end of paper). A true increase in the buckling strength of Z- and I-section panels would therefore require a very significant increase above the strength of T-section panels. Table 6 shows that only the FEA approach predicts such a significant increase in buckling strength.

The FEA results shown in Table 6 also support the hypothesis that a heavy attached flange allows load to be more effectively redirected to the stiffeners. When the stiffener strength is increased, the performance gap between the T- and I-section panels widens from 42% for 6056 stiffeners to almost 61% for next-generation 7xxx stiffeners. Since the increase in cross-sectional area between the two designs is less than 51%, as shown in Table 5, the overall efficiency of the panels with large fastened flanges is clearly increased.

The correlation between the predictions of the FEA method and the hypotheses of the present work is not reflected in the results of the Euler-Johnson method. This discrepancy is attributed to the inability of the implementation of the Euler-Johnson method used for these calculations to account for skin-stiffener bending-twisting coupling and other effects that impact panel buckling. Future work will include a detailed investigation into the improvements necessary in order to achieve accurate predictions and experimental validation.

Conclusions

FEA has shown that, given a perfect joint between skin and stiffeners and strong enough stiffener material, the overall efficiency of a stiffened panel with large

attached flanges is greater than that of a panel with a very high quadratic section moment. Stiffener pitches can thus be kept at economic levels while panel buckling performance is improved through the use of new high-strength, damage-tolerant skin and the next generation of high-strength stiffeners. An attempt was made to develop a special implementation of the Euler-Johnson method to predict these results, but this effort has not yet produced satisfactory results.

The tangent modulus curves of the next generation of high-strength stiffener materials can generally be expected to be steeper than those of current materials. The present analyses have demonstrated that because the strain in a post-buckled stiffened panel is non-uniform, this does not present any particular risks with respect to sudden loss of stiffness of the panel.

References

1. Bruhn, E.F., et. al., *Analysis and Design of Flight Vehicle Structures*, Jacobs Publishing, Indianapolis, 1973.

2. Niu, M.C.Y., *Airframe Stress Analysis and Sizing*, Second Edition, Hong Kong Conmilit Press, Hong Kong, 1999.

3. Lynch, C., Sterling, S., *A Finite Element Study of the Postbuckling Behaviour of a Flat Stiffened Panel*, 21st ICAS Congress, Melbourne, 1998.

	ts	*bs*	*tff*	*blff*	*brff*	*tw*	*h*	*tf*	*blf*	*brf*
T 0.208	2.25	203.2				1.25	40.35	3	12.075	12.075
Z 0.316	2.25	203.2	3.5		36.85	1.25	40.35	3	11.45	
Z 0.347	2.25	203.2	3.5		35.85	2.25	40.35	3	10.45	
I 0.455	2.25	203.2	3.5	37.475	35.85	2.25	40.35	3	10.45	

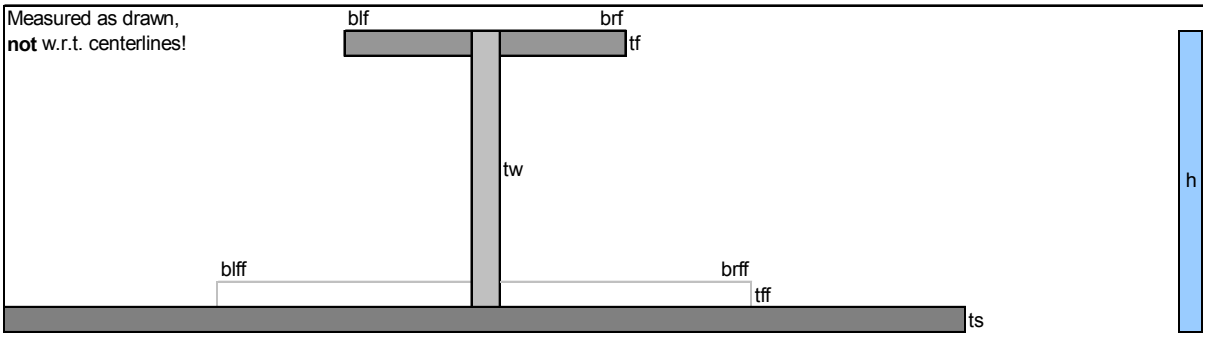

All dimensions in mm

Table 1: Dimensions of panel cross-sections analyzed

Stiffener	Material	Stiffening Ratio ($A_{stiffener}/A_{total}$)	Skin Crippling Stress (MPa)	Average Panel Stress @ Ultimate Load (MPa)
T	6056	0.208	-31	-128
	7349			-153
	Next generation 7xxx			-162
Z	6056	0.316	-31	-117
	7349			-131
	Next generation 7xxx			-134
	6056	0.347		-128
	7349			-149
	Next generation 7xxx			-157
I	6056	0.455	-31	-140
	7349			-160
	Next generation 7xxx			-166

Table 2: Critical stresses from Euler-Johnson analyses with no bond modeled between skin and stiffeners

Stiffener	Material	Stiffening Ratio ($A_{stiffener}/A_{total}$)	Skin Crippling Stress (MPa)	Average Panel Stress @ Ultimate Load (MPa)
T	6056	0.208	-31	-130
	7349			-156
	Next generation 7xxx			-166
Z	6056	0.316	-47	-152
	7349			-169
	Next generation 7xxx			-171
	6056	0.347		-162
	7349			-184
	Next generation 7xxx			-187
I	6056	0.455	-79	-204
	7349			-231
	Next generation 7xxx			-235

Table 3: Critical stresses from Euler-Johnson analyses with a perfect bond modeled between skin and stiffeners

Stiffener	Material	Stiffening ratio ($A_{stiffener}/A_{total}$)	Average panel stress @ first loss of stiffness (MPa)	Average panel stress @ ultimate load (MPa)
T	6056	0.208	-47	-147
	7349			-163
	Next generation 7xxx			-166
Z	6056	0.316	-58	-155
	7349			-173
	Next generation 7xxx			-176
	6056	0.347	-67	-183
	7349			-211
	Next generation 7xxx			-223
I	6056	0.455	-83	-209
	7349			247
	Next generation 7xxx			267

Table 4: Critical stresses from FEA models

Stiffener	Stiffening ratio ($A_{stiffener}/A_{total}$)	Total section per stiffener bay (mm^2)	Increase of section
T	0.208	577	
Z	0.316	668	19.9%
	0.347	700	25.7%
I	0.455	840	50.8%

Table 5: Cross-sections of the different designs

Stiffener	Material	Stiffening ratio ($A_{stiffener}/A_{total}$)	E-J "free"	E-J perfect bond	FEA
T	6056	0.208			
	7349				
	Next generation 7xxx				
Z	6056	0.316	-8.6%	16.9%	5.4%
	7349		-14.4%	8.3%	6.1%
	Next generation 7xxx		-17.3%	3.0%	6.0%
	6056	0.347	0.0%	24.6%	24.5%
	7349		-2.6%	17.9%	29.4%
	Next generation 7xxx		-3.1%	12.7%	34.3%
I	6056	0.455	9.4%	56.9%	42.2%
	7349		4.6%	48.1%	51.5%
	Next generation 7xxx		2.5%	41.6%	60.8%

Table 6: Changes in panel buckling strength with respect to T-stiffened design predicted by the three calculation methods.

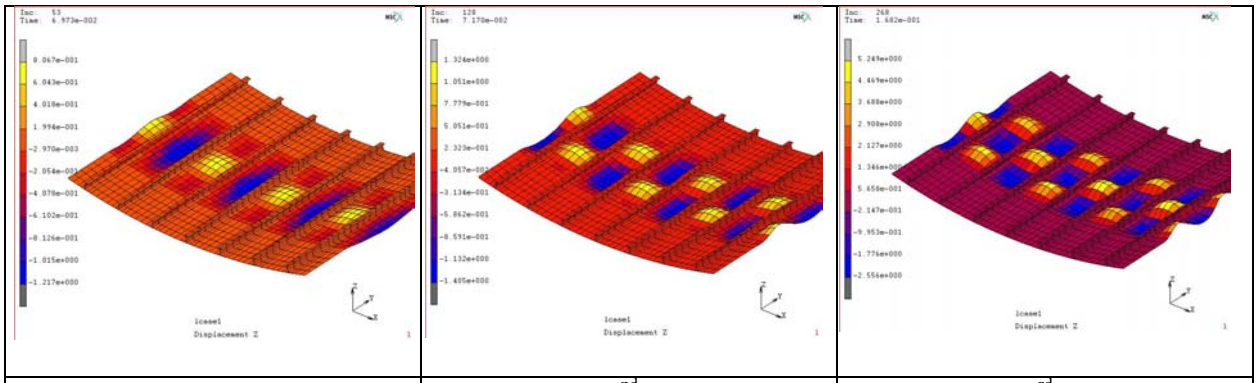

Out-of-plane displacements magnified 25x, 1st buckling mode observed	10x, 2nd mode	10x, 3rd mode

Figure 3: Successive buckling modes of the T-stiffened panel calculated by FEA

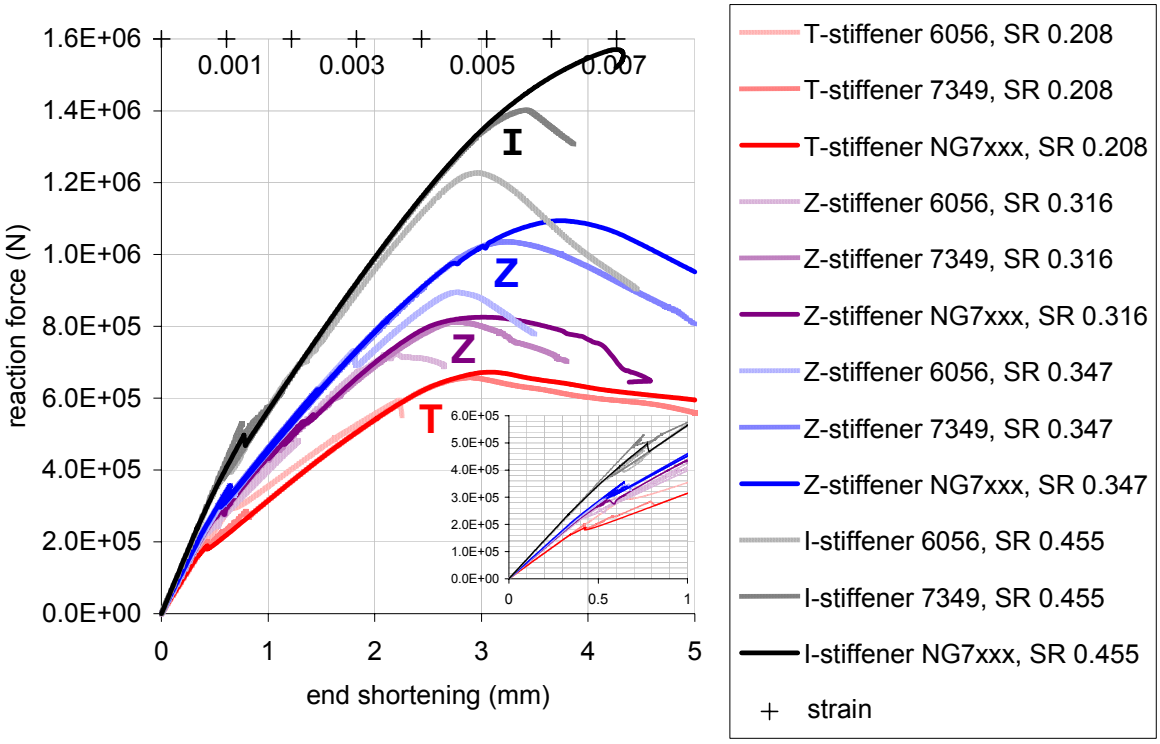

Figure 4: Force-displacement curves from FEA models, including a zoom on the area in which the panels first lose their stiffness. A second horizontal axis gives the average strain in the panels.